Galileons and Naked Singularities

Thomas Curtright, University of Miami

FAU seminar, 14 November 2012

Spherically symmetric solutions of hypothetical scalar field "galileon" models will be discussed in the context of general relativity. There are two distinct phases of solutions arising from physically reasonable boundary conditions. Those in the "censored" phase exhibit horizons, as expected, while those in the "naked" phase have curvature singularities without horizons.

Based on arXiv:1206.3616 [hep-th], arXiv:1208.1205 [hep-th], and unpublished work in collaboration with David Fairlie, University of Durham.

Je n'ai fait celle-ci plus longue que parce que je n'ai pas eu le loisir de la faire plus courte.
B Pascal, *Lettres Provinciales XVI* (1656)

Galileon theories are a class of models for hypothetical scalar fields whose Lagrangians involve multilinears of first and second derivatives, but whose nonlinear field equations are still only second order. They may be important for the description of large-scale features in astrophysics as well as for elementary particle theory. Hierarchies of galileon Lagrangians were discussed mathematically for flat spacetime, independently of an earlier systematic survey of second-order scalar-tensor field equations in curved 4D spacetime. The simplest example involves a single scalar field, ϕ. This galileon field may be coupled "universally" to the trace of the energy-momentum tensor, Θ, and upon so doing, it is gravitation-like by virtue of the similarity between this universal coupling and that of the metric $g_{\mu\nu}$ to $\Theta_{\mu\nu}$ in general relativity. As might be expected from this similarity and the ubiquitous generation of scalar fields by the process of dimensional reduction, it is possible to obtain some galileon models from limits of higher dimensional gravitation theories. Indeed, galileon models were discovered yet again by this process.

$$A = \int \phi_\alpha \phi_\alpha \ \phi_{\beta\beta} \ d^n x \tag{1}$$

where ϕ is the scalar galileon field, $\phi_\alpha = \partial\phi(x)/\partial x^\alpha$, etc., and where repeated indices are summed using the Lorentz metric $\delta_{\mu\nu} = \mathrm{diag}(1, -1, -1, \cdots)$. The field equations are $\mathcal{E} = 0$ where

$$\frac{\delta A}{\delta \phi} = -2\ \mathcal{E} \tag{2}$$

$$\mathcal{E} = \phi_{\alpha\alpha}\phi_{\beta\beta} - \phi_{\alpha\beta}\phi_{\alpha\beta} \tag{3}$$

More generally, there is a hierarchy for $1 \leq k \leq n$.

$$\mathcal{A}_k = \int \phi_\alpha \phi_\alpha \ \mathcal{E}_{k-1} \ d^n x \tag{4}$$

$$\mathcal{E}_{k-1} = \delta^{\alpha_1\alpha_2\cdots\alpha_{k-1}}_{\beta_1\beta_2\cdots\beta_{k-1}} \times \phi_{\alpha_1\beta_1}\phi_{\alpha_2\beta_2}\cdots\phi_{\alpha_{k-1}\beta_{k-1}} \tag{5}$$

Effects of $\phi\ \Theta[\phi]$ self-couplings

Consider the classical features of galileon theories with an additional self-coupling of the fields to the trace of their own energy-momentum tensor, in flat 4D spacetime.

For the simplest example, the galileon field is usually coupled to all *other* matter through the trace of the energy-momentum tensor, $\Theta^{(\text{matter})}$. But *surely*, in a self-consistent theory the galileon should also be coupled to its own energy-momentum trace, even in the flat spacetime limit. Some consequences of this additional self-coupling are considered here.

Non-vanishing trace

Including in A a minimal coupling to a background spacetime metric yields a symmetric energy-momentum tensor, which becomes in the flat-space limit:

$$\Theta_{\mu\nu}^{(2)} = \phi_\mu \phi_\nu \phi_{\alpha\alpha} - \phi_\alpha \phi_{\alpha\nu} \phi_\mu - \phi_\alpha \phi_{\alpha\mu} \phi_\nu + \delta_{\mu\nu} \phi_\alpha \phi_\beta \phi_{\alpha\beta} \ . \tag{6}$$

This is seen to be conserved,

$$\partial_\mu \Theta_{\mu\nu}^{(2)} = \phi_\nu \ \mathcal{E}_2 [\phi] \ , \tag{7}$$

upon using the field equation that follows from locally extremizing A, $0 = \delta A / \delta\phi = -\mathcal{E}_2 [\phi]$, where

$$\mathcal{E}_2 [\phi] \equiv \phi_{\alpha\alpha} \phi_{\beta\beta} - \phi_{\alpha\beta} \phi_{\alpha\beta} \ . \tag{8}$$

Now, this $\Theta_{\mu\nu}^{(2)}$ is not traceless. Consequently, the usual form of the scale current, $x_\alpha \Theta_{\alpha\mu}^{(2)}$, is not conserved. On the other hand, the action (1) is homogeneous in ϕ and its derivatives, and is clearly invariant under the scale transformations $x \to sx$ and $\phi(x) \to s^{(4-n)/3} \phi(sx)$. Hence the corresponding Noether current must be conserved. This current is easily found, especially for $n = 4$, so let us restrict our attention to four spacetime dimensions in the following.

In that case the trace is obviously a total divergence:

$$\Theta^{(2)} \equiv \delta_{\mu\nu}\Theta^{(2)}_{\mu\nu} = \partial_\alpha \left(\phi_\alpha \phi_\beta \phi_\beta\right) \ . \tag{9}$$

That is to say, for $n = 4$ the virial is the trilinear $V_\alpha = \phi_\alpha \phi_\beta \phi_\beta$. So a conserved scale current is given by the combination,

$$S_\mu = x_\alpha \Theta^{(2)}_{\alpha\mu} - \phi_\alpha \phi_\alpha \phi_\mu \ . \tag{10}$$

Interestingly, this virial is not a divergence modulo a conserved current, so this model is *not* conformally invariant despite being scale invariant. Be that as it may, it is not our principal concern here.

Our interest here is that the nonzero trace suggests an additional interaction where ϕ couples directly to its own $\Theta^{(2)}$. This is similar to coupling a conventional *massive* scalar to the trace of its own energy-momentum tensor. In that previously considered example, however, the consistent coupling of the field to its trace required an iteration to all orders in the coupling. Upon summing the iteration and making a field redefinition, the Nambu-Goldstone model emerged. But, for the simplest galileon model in four spacetime dimensions, (1), a consistent coupling of field and trace is much easier to implement. *No iteration is required.* The first-order coupling alone is consistent, after integrating by parts and ignoring boundary contributions, so that

$$-\tfrac{1}{4}\int \phi\ \partial_\alpha \left(\phi_\alpha \phi_\beta \phi_\beta\right)\ d^4x = \tfrac{1}{4}\int \phi_\alpha \phi_\alpha \phi_\beta \phi_\beta\ d^4x \ . \tag{11}$$

Consistency follows because (11) gives an additional contribution to the energy-momentum tensor which is *traceless*, in 4D spacetime:

$$\Theta^{(3)}_{\mu\nu} = \phi_\mu \phi_\nu \phi_\alpha \phi_\alpha - \tfrac{1}{4}\delta_{\mu\nu}\phi_\alpha \phi_\alpha \phi_\beta \phi_\beta \ , \quad \Theta^{(3)} = 0 \ . \tag{12}$$

Coupling ϕ to its own trace may impact the Vainstein mechanism by changing the effective coupling of $\Theta^{(\text{matter})}$ to both backgrounds and fluctuations in ϕ. But we leave this as an exercise.

A model with additional quartic self-coupling

Based on these elementary observations, we consider a model with action

$$A = \int \left(\tfrac{1}{2}\phi_\alpha \phi_\alpha - \tfrac{1}{2}\lambda \phi_\alpha \phi_\alpha \phi_{\beta\beta} - \tfrac{1}{4}\kappa \phi_\alpha \phi_\alpha \phi_\beta \phi_\beta \right) \, d^4x \ , \tag{13}$$

where for the Lagrangian L we take a mixture of three terms: the standard bilinear, the trilinear galileon, and its corresponding quadrilinear trace-coupling. The quadrilinear is reminiscent of the Skyrme term in nonlinear σ models although here the topology would appear to be always trivial.

The second and third terms in A are logically connected, as we have indicated. But why include in A the standard bilinear term? The reasons for including this term are to soften the behavior of solutions at large distances, as will be evident below, and also to satisfy Derrick's criterion for classical stability under the rescaling of x. Without the bilinear term in L the energy within a spatial volume would be neutrally stable under a uniform rescaling of x, and therefore able to disperse.

Similarly, for positive κ, the last term in A ensures the energy density of static solutions is always bounded below under a rescaling of the field ϕ, a feature that would not be true if $\kappa = 0$ but $\lambda \neq 0$. So, we only consider $\kappa > 0$ in the following. But before discussing the complete $\Theta_{\mu\nu}$ for the model, we note that we did *not* include in A a term coupling ϕ to the trace of the energy-momentum due to the standard bilinear term, namely, $\int \phi \Theta^{(1)} d^4x$, where

$$\Theta^{(1)}_{\mu\nu} = \phi_\mu \phi_\nu - \tfrac{1}{2}\delta_{\mu\nu}\phi_\alpha \phi_\alpha \ , \quad \Theta^{(1)} = -\phi_\alpha \phi_\alpha \ . \tag{14}$$

We have omitted such an additional term in A solely as a matter of taste, thereby ensuring that L is invariant under constant shifts of the field. Among other things, this greatly simplifies the task of finding solutions to the equations of motion.

The field equation of motion for the model is $0 = \delta A/\delta\phi = -\mathcal{E}[\phi]$, where

$$\mathcal{E}[\phi] \equiv \phi_{\alpha\alpha} - \lambda\left(\phi_{\alpha\alpha}\phi_{\beta\beta} - \phi_{\alpha\beta}\phi_{\alpha\beta}\right) - \kappa\left(\phi_\alpha\phi_\beta\phi_\beta\right)_\alpha \ . \tag{15}$$

As expected, this field equation is second-order, albeit nonlinear. Also note, under a rescaling of both x and ϕ, nonzero parameters λ and κ can be scaled out of the equation. Define

$$\phi(x) = \frac{\lambda}{\kappa}\,\psi\left(\sqrt{\frac{\kappa}{\lambda^2}}x\right) \ . \tag{16}$$

Then the field equation for $\psi(z)$ becomes

$$\psi_{\alpha\alpha} - \left(\psi_{\alpha\alpha}\psi_{\beta\beta} - \psi_{\alpha\beta}\psi_{\alpha\beta}\right) - \left(\psi_\alpha\psi_\beta\psi_\beta\right)_\alpha = 0\ , \tag{17}$$

where $\psi_\alpha = \partial\psi(z)/\partial z^\alpha$, etc. In effect then, if both λ and κ do not vanish, it is only necessary to solve the model's field equation for $\lambda = \kappa = 1$.

Static solutions

For static, spherically symmetric solutions, $\phi = \phi(r)$, the field equation of motion becomes

$$0 = \frac{1}{r^2}\frac{d}{dr}\left(r^2\left(\phi' + \lambda\frac{2}{r}(\phi')^2 + \kappa(\phi')^3\right)\right) \ . \tag{18}$$

where $\phi' = d\phi/dr$. This is immediately integrated once to obtain a cubic equation,

$$r^2\phi' + 2\lambda r(\phi')^2 + \kappa r^2(\phi')^3 = C \ , \tag{19}$$

where C is the constant of integration. Now, without loss of generality (cf. (16) and (17)) we may choose $\lambda > 0$. Then, if $C = 0$, either ϕ' vanishes, or else there are two solutions that are real only within a finite sphere of radius $r = \sqrt{\lambda^2/\kappa}$. These two "interior" solutions are given exactly by

$$\phi'_{\pm} = -\frac{1}{r\kappa}\left(\lambda \pm \sqrt{\lambda^2 - r^2\kappa}\right) \ . \tag{20}$$

Note that these solutions always have $\phi' < 0$ within the finite sphere.

Otherwise, if $C \neq 0$, then examination of the cubic equation for small and large $|\phi'|$ determines the asymptotic behavior of ϕ' for large and small r. In particular, there is only one type of asymptotic behavior for large r:

$$\phi' \underset{r\to\infty}{\sim} \frac{C}{r^2} \quad \text{for either sign of } C \ . \tag{21}$$

However, there are two types of behavior for large $|\phi'|$, corresponding to small r. The solutions which are real for all $r > 0$ have small and large r behavior given by either

$$\phi' \underset{r \to 0}{\sim} \sqrt{\frac{C}{2\lambda r}} \quad \text{and} \quad \phi' \underset{r \to \infty}{\sim} \frac{C}{r^2} \quad \text{for } C > 0, \tag{22}$$

or else

$$\phi' \underset{r \to 0}{\sim} \frac{-2\lambda}{\kappa r} \quad \text{and} \quad \phi' \underset{r \to \infty}{\sim} \frac{C}{r^2} \quad \text{for } C < 0. \tag{23}$$

From further inspection of the cubic equation to determine the behavior of ϕ' for intermediate values of r, when $C > 0$ it turns out that ϕ' is a single-valued, positive function for all $r > 0$, joining smoothly with the asymptotic behaviors given in (22). However, it also turns out there is an additional complication when $C < 0$. In this case there is a critical value $\left(\kappa^{3/2}/\lambda^2\right) C_{\text{critical}} = -4\sqrt{3}/27 \approx -0.2566$ such that, if $C \leq C_{\text{critical}}$ then ϕ' is a single-valued, negative function for all $r > 0$, while if $C_{\text{critical}} < C < 0$ then ϕ' is triple-valued for an open interval in $r > 0$. It is not completely clear to us what physics underlies this multivalued-ness for some negative C. But in any case, when $C < 0$ it is also true that ϕ' joins smoothly with the asymptotic behaviors given in (23). All this is illustrated in Figures 1 and 2, for $\lambda = \kappa = 1$.

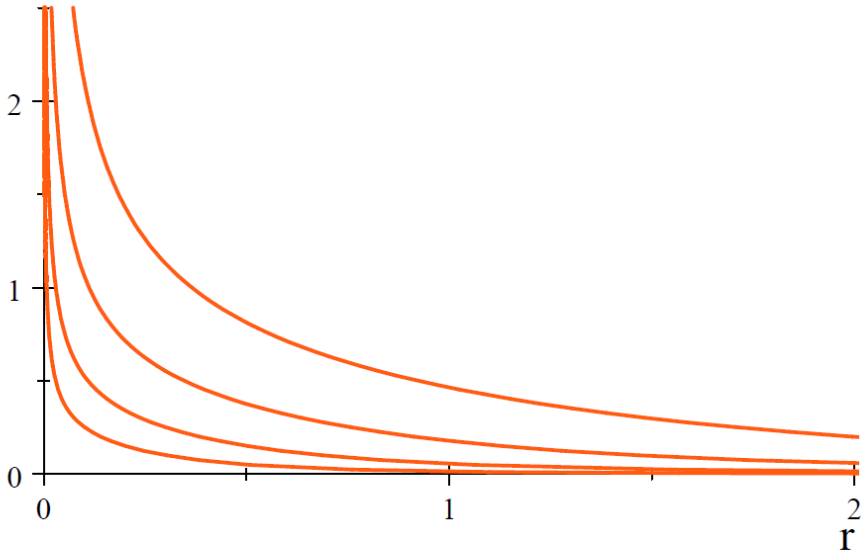

$\psi'(r)$ for $C = +1/4^N$, with $N = 0, 1, 2, 3$ for top to bottom curves, respectively.

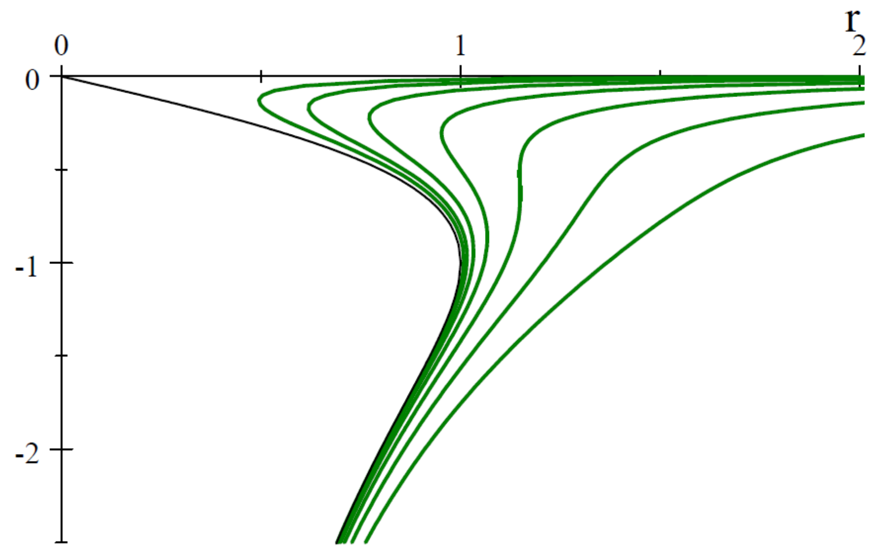

$\psi'(r)$ for $C = -1/2^N$, with $N = 6, 5, 4, 3, 2, 1, 0$ from left to right, respectively. The thin black curve is a union of the two $C = 0$ solutions in (20).

For the solutions described by (22) and (23), the total energy outside any large radius is obviously finite for both $C > 0$ and $C < 0$. And if $C > 0$, the total energy within a small sphere surrounding the origin is also manifestly finite. But if $C < 0$ the energy within that same small sphere could be infinite *unless* there is a cancellation between the galileon term and the trace interaction term. Remarkably, this cancellation does occur. So both $C > 0$ and $C < 0$ static solutions for the model have finite total energy.

Energy considerations

Complete information about the distribution of energy is provided by the model's energy-momentum tensor,

$$\Theta_{\mu\nu} = \Theta^{(1)}_{\mu\nu} - \lambda\Theta^{(2)}_{\mu\nu} - \kappa\Theta^{(3)}_{\mu\nu} \ . \tag{24}$$

As expected, this is conserved, given the field equation $\mathcal{E}\left[\phi\right] = 0$, since

$$\partial_\mu \Theta_{\mu\nu} = \phi_\nu \mathcal{E}\left[\phi\right] \ . \tag{25}$$

The energy density for *static* solutions differs from the canonical energy density for such solutions (namely, $-L$) by a total spatial divergence that arises from the galileon term:

$$\Theta_{00} = -\left. L\right|_{\text{static}} - \tfrac{1}{2}\lambda\overrightarrow{\nabla}\cdot\left(\left(\nabla\phi\right)^2\overrightarrow{\nabla}\phi\right) \ . \tag{26}$$

This divergence will not contribute to the total energy for fields such that $\lim_{r\to\infty}\left(\phi/\ln r\right)$ exists. Assuming that is the case, Derrick's scaling argument for static, finite energy solutions of the equations of motion shows the energy is just twice that due to the bilinear $\Theta^{(1)}_{00}$. Thus,

$$E = \int \Theta_{00}\, d^3r = \int \left(\overrightarrow{\nabla}\phi\right)^2\, d^3r \ . \tag{27}$$

For the spherically symmetric static solutions of (19), this becomes an expression of the energy as a function of the parameters and the constant of integration C:

$$E\left[\lambda,\kappa,C\right]=4\pi\int_{0}^{\infty}\left(\phi'\right)^{2}\ r^{2}dr\ . \tag{28}$$

Again without loss of generality, consider $\lambda=\kappa=1$. Then for either $C>0$ or for $C<C_{\text{critical}}<0$, change integration variables from r to $s\equiv\phi'$ to find:[1]

$$E\left(C\gtrless0\right)=I\left(\left|C\right|\right)\mp\left(\left|C\right|+\tfrac{1}{2}\pi\right)\ , \tag{29}$$

$$I\left(C>0\right)\equiv\tfrac{1}{2}\int_{0}^{\infty}\frac{P\left(s,C\right)\ ds}{\left(s^{2}+1\right)^{4}\sqrt{s^{4}+s\left(s^{2}+1\right)C}}\ , \tag{30}$$

where the numerator of the integrand is an eighth-order polynomial in s, namely,

$$P\left(s,C\right)=8s^{8}+12Cs^{7}+\left(3C^{2}-8\right)s^{6}+8Cs^{5}+7C^{2}s^{4}-4Cs^{3}+5C^{2}s^{2}+C^{2}\ . \tag{31}$$

Thus, $I\left(C\right)$ is an elliptic integral. But rather than express the final result in terms of standard functions, it suffices here just to plot $E\left(C\right)$, in Figure 3. Note that E increases monotonically with $\left|C\right|$.

[1] The multivalued behavior of any solution for $C_{\text{critical}}<C<0$ makes the determination of the total energy ambiguous, at best, for these cases. This is an unresolved issue.

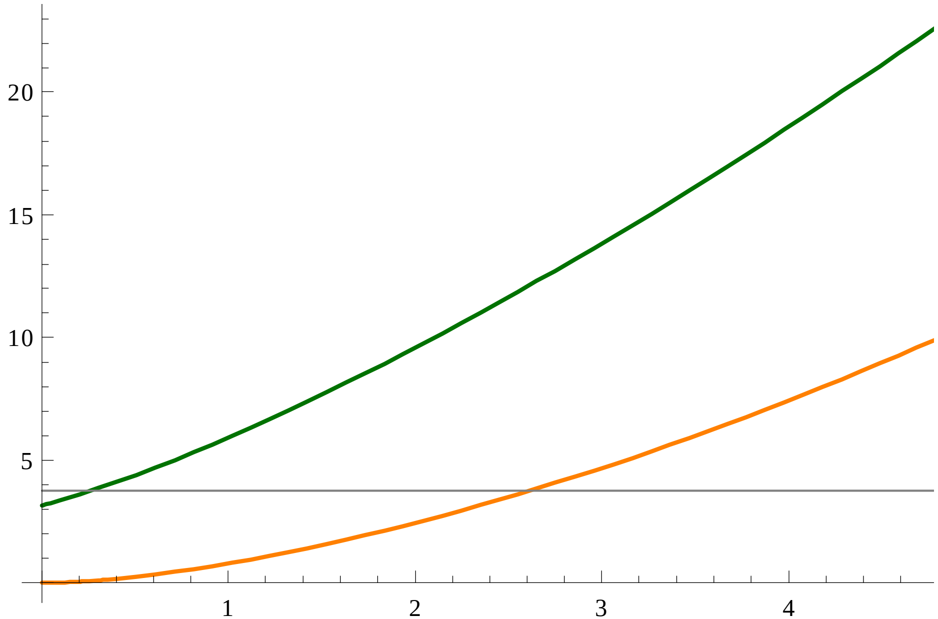

$E\left(\pm C\right)$ versus $C \geq 0$ as lower/upper curves (the horizontal line is $E\left(C_{\text{critical}}\right) \approx 3.7396$).

For other values of λ and κ with the constant of integration C specified as in (19), the energy of the solution is given in terms of the function defined by (29,30):

$$E\left[\lambda, \kappa, C\right] = \left(\lambda^3/\kappa^{5/2}\right) \ E\left(\kappa^{3/2} C/\lambda^2\right) \ . \tag{32}$$

The energy curves indicate double degeneracy in E, for different values of $|C|$, when $E\left[\lambda, \kappa, C\right] > \pi\lambda^3/\kappa^{5/2}$. Also, for a given $|C|$ the negative C solutions are *higher* in energy, with $E\left[\lambda, \kappa, -\left|C\right|\right] - E\left[\lambda, \kappa, \left|C\right|\right] = \pi\lambda^3/\kappa^{5/2} + 2\left|C\right|\lambda/\kappa$. Or at least this is true for all $|C| \geq |C_{\text{critical}}|$ in which case $E\left[\lambda, \kappa, C\right] \geq \frac{\lambda^3}{\kappa^{5/2}} E\left(\frac{\kappa^{3/2}}{\lambda^2} C_{\text{critical}}\right) \approx 3.7396 \ \lambda^3/\kappa^{5/2}$.

A test particle coupled by $\phi\Theta^{(\mathrm{matter})}$ to any of these galileon field configurations would see an effective potential which is not $1/r$, for intermediate and small r. Therefore its orbit would show deviations from the usual Kepler laws, including precession that is possibly at variance with the predictions of conventional general relativity. It would be interesting to search for such effects, say, by considering stars orbiting around the galactic center. In fact, experimenters have been engaged in searches of this type for some time ...

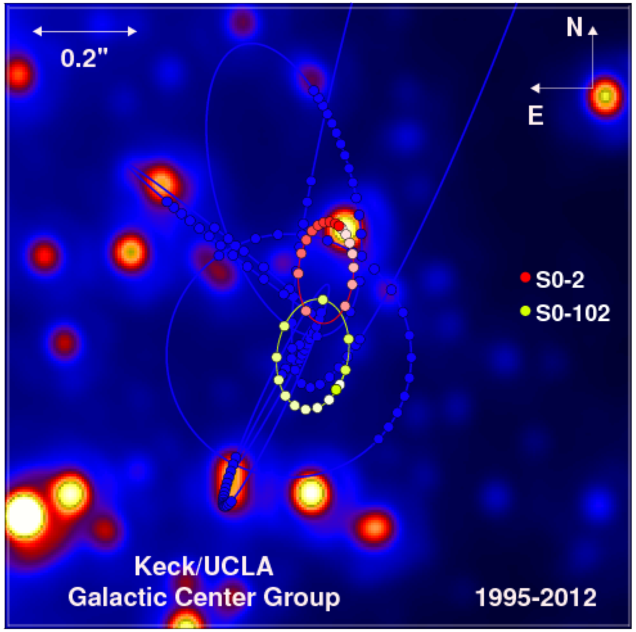

Webpage
Video

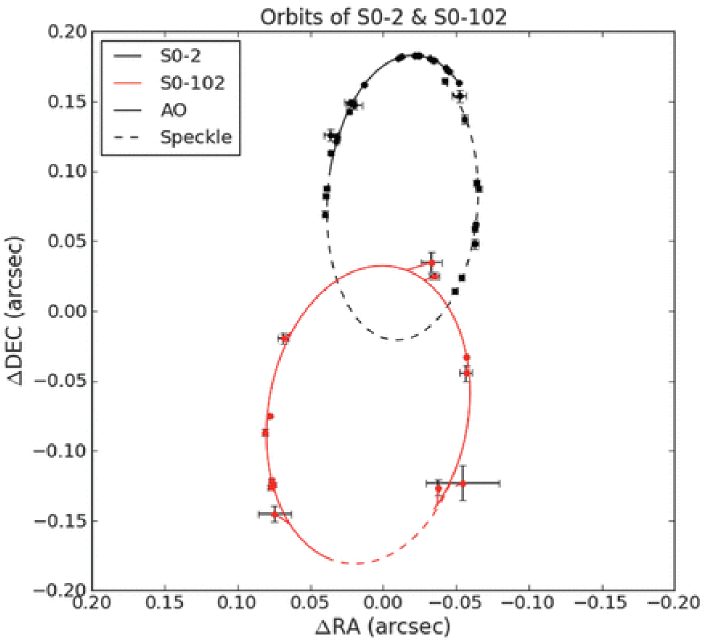

From Ghez et al., *The Shortest-Known–Period Star Orbiting Our Galaxy's Supermassive Black Hole,* Science 5 October 2012: vol. 338 no. 6103 pp 84-87. The orbits of S0-2 (black) and S0-102 (red). RA, right ascension; DEC, declination. Both stars orbit clockwise. The data points for S0-2 range from the year 1995 to 2012, and S0-102's detections range from 2000 to 2012. Although the best-fit orbits are not closing, the statistically allowed sets of orbital trajectories are consistent with a closed orbit. S0-102 has an orbital period of 11.5 years, 30% shorter than that of S0-2.

Science article

Supplementary material

$d = \frac{0.4}{360\times60\times60} \times 2\pi \times 27000 = 0.05$ ly

General relativistic effects

If the simple trace-coupled Galileon model is coupled minimally to gravitation (GR) the resulting system admits spherically symmetric static solutions with naked spacetime curvature singularities.

We have discussed the effects of coupling a Galileon to its own energy-momentum trace in the flat spacetime limit. Here, general relativistic effects are taken into consideration and additional features of this same model are explored in curved spacetime. The main point to be emphasized is that there can be solutions with *naked singularities* when the energy in the scalar field is finite and not too large, and for which the effective mass of the system is positive. Thus for the simple model at hand there is an open set of *physically acceptable* scalar field data for which curvature singularities are *not* hidden inside event horizons. This would seem to have important implications for the cosmic censorship conjecture of Penrose. It is worthwhile to note that, in general, naked singularities have observable consequences that differ from those due to black holes.

Minimal coupling to gravity

The scalar field part of the action in curved space is

$$A = \frac{1}{2} \int g^{\alpha\beta} \phi_\alpha \phi_\beta \left(1 - \frac{1}{\sqrt{-g}}\, \partial_\mu \left(\sqrt{-g} g^{\mu\nu} \phi_\nu\right) - \frac{1}{2}\, g^{\mu\nu} \phi_\mu \phi_\nu\right) \sqrt{-g}\ d^4x\ . \tag{33}$$

This gives a symmetric energy-momentum tensor $\Theta_{\alpha\beta}$ for ϕ upon variation of the metric.

$$\delta A = \tfrac{1}{2} \int \sqrt{-g}\ \Theta_{\alpha\beta}\ \delta g^{\alpha\beta}\ d^4x\ , \tag{34}$$

$$\begin{aligned} \Theta_{\alpha\beta} = {} & \phi_\alpha \phi_\beta \left(1 - g^{\mu\nu} \phi_\mu \phi_\nu\right) - \tfrac{1}{2} g_{\alpha\beta}\ g^{\mu\nu} \phi_\mu \phi_\nu \left(1 - \tfrac{1}{2} g^{\rho\sigma} \phi_\rho \phi_\sigma\right) \\ & - \phi_\alpha \phi_\beta \tfrac{1}{\sqrt{-g}} \partial_\mu \left(\sqrt{-g} g^{\mu\nu} \phi_\nu\right) + \tfrac{1}{2} \partial_\alpha \left(g^{\mu\nu} \phi_\mu \phi_\nu\right) \phi_\beta + \tfrac{1}{2} \partial_\beta \left(g^{\mu\nu} \phi_\mu \phi_\nu\right) \phi_\alpha - \tfrac{1}{2} g_{\alpha\beta} \partial_\rho \left(g^{\mu\nu} \phi_\mu \phi_\nu\right) g^{\rho\sigma} \phi_\sigma\ . \end{aligned} \tag{35}$$

It also gives the field equation for ϕ upon variation of the scalar field, $\mathcal{E}[\phi]=0$, where

$$\delta A=-\int\sqrt{-g}\;\mathcal{E}[\phi]\;\;\delta\phi\;d^4x\;, \tag{36}$$

$$\mathcal{E}[\phi]=\partial_\alpha\left[g^{\alpha\beta}\phi_\beta\sqrt{-g}-g^{\alpha\beta}\phi_\beta\;g^{\mu\nu}\phi_\mu\phi_\nu\sqrt{-g}-g^{\alpha\beta}\phi_\beta\partial_\mu\left(\sqrt{-g}g^{\mu\nu}\phi_\nu\right)+\tfrac{1}{2}\sqrt{-g}g^{\alpha\beta}\partial_\beta\left(g^{\mu\nu}\phi_\mu\phi_\nu\right)\right]\;. \tag{37}$$

Since $\mathcal{E}[\phi]$ is a total divergence, it easily admits a first integral for static, spherically symmetric configurations. Consider *only* those situations in the following.

Static spherical solutions

For such configurations the metric in generalized Schwarzschild coordinates is

$$(ds)^2=e^{N(r)}(dt)^2-e^{L(r)}(dr)^2-r^2(d\theta)^2-r^2\sin^2\theta\,(d\varphi)^2\;. \tag{38}$$

Thus for static, spherically symmetric ϕ, with covariantly conserved energy-momentum tensor (35), Einstein's equations reduce to just a pair of coupled 1st-order nonlinear equations:

$$r^2\Theta_t{}^t=e^{-L}\left(rL'-1\right)+1\;, \tag{39}$$

$$r^2\Theta_r{}^r=e^{-L}\left(-rN'-1\right)+1\;. \tag{40}$$

These are to be combined with the first integral of the ϕ field equation in this situation. Defining

$$\eta(r)\equiv e^{-L(r)/2}\;,\qquad \varpi(r)\equiv\eta(r)\,\phi'(r)\;\;, \tag{41}$$

that first integral becomes

$$\frac{Ce^{-N/2}}{r^2}=\varpi\left(1+\varpi^2\right)+\frac{1}{2}\left(N'+\frac{4}{r}\right)\eta\varpi^2\;, \tag{42}$$

where for asymptotically flat spacetime the constant C is given by $\lim_{r\to\infty} r^2\phi'(r) = C$. Then upon using

$$\Theta_t{}^t = \Theta_\theta{}^\theta = \Theta_\varphi{}^\varphi = \tfrac{1}{2}\varpi^2\left(1+\tfrac{1}{2}\varpi^2\right) - \eta\varpi^2\varpi' \ , \tag{43}$$
$$\Theta_r{}^r = -\tfrac{1}{2}\varpi^2\left(1+\tfrac{3}{2}\varpi^2\right) - \tfrac{1}{2}\eta\varpi^3\left(N'+\tfrac{4}{r}\right) \ , \tag{44}$$

the remaining steps to follow are clear.

First, for $C\neq 0$, one can eliminate N' from (40) and (42) to obtain an exact expression for N in terms of η, ϖ, and C:

$$e^{N/2} = \frac{8C}{r\varpi}\frac{\eta-\frac{1}{2}r\varpi^3}{\left(4\varpi-2r^2\varpi^3-r^2\varpi^5+8r\eta+12\varpi\eta^2+8r\varpi^2\eta\right)} \ . \tag{45}$$

(cf. the lapse function, $\mathcal{N} = e^{N/2}$) If the numerator of this last expression vanishes there is an *event horizon*, otherwise not. When $\eta = \frac{1}{2}r\varpi^3$ the denominator of (45) is positive definite.

Next, in addition to (39) one can now eliminate N from either (40) or (42) to obtain two coupled first-order nonlinear equations for η and ϖ. These can be integrated, at least numerically. Or they can be used to determine analytically the large and small r behaviors, hence to see if the energy and curvature are finite. For example, again for asymptotically flat spacetime, it follows that

$$e^{L/2} \underset{r\to\infty}{\sim} 1+\frac{M}{r}+\frac{1}{4}\left(6M^2-C^2\right)\frac{1}{r^2}+\frac{1}{2}M\left(5M^2-2C^2\right)\frac{1}{r^3}+O\left(\frac{1}{r^4}\right) \ , \tag{46}$$
$$e^{N/2} \underset{r\to\infty}{\sim} 1-\frac{M}{r}-\frac{1}{2}M^2\frac{1}{r^2}+\frac{1}{12}M\left(C^2-6M^2\right)\frac{1}{r^3}+O\left(\frac{1}{r^4}\right) \ , \tag{47}$$
$$\varpi \underset{r\to\infty}{\sim} \frac{C}{r^2}\left(1+\frac{M}{r}+\frac{3}{2}M^2\frac{1}{r^2}\right)+O\left(\frac{1}{r^5}\right) \ , \tag{48}$$

for constant C and M.

To date the details of the two remaining first-order ordinary differential equations are not pretty, but the equations are numerically tractable. In terms of the variables defined in (41), in light of (45), Einstein's equation (40) becomes

$$F\left(r,\varpi,\eta\right)r\frac{d}{dr}\varpi+G\left(r,\varpi,\eta\right)r\frac{d}{dr}\eta=H\left(r,\varpi,\eta\right)\ , \tag{49}$$

$$\begin{aligned} F\left(r,\varpi,\eta\right)&=-4\eta\left[2r^3\varpi^6+3r^3\varpi^8+16\varpi\eta+4r\varpi^4\right.\\ &\quad\left.+16r\eta^2+48\varpi\eta^3+48r\varpi^2\eta^2+12r\varpi^4\eta^2-12r^2\varpi^5\eta\right]\ , &(50)\\ G\left(r,\varpi,\eta\right)&=8\eta\varpi^2\left[2r^2\varpi^2+3r^2\varpi^4-12\eta^2+12r\varpi^3\eta+4\ \right]\ , &(51)\\ H\left(r,\varpi,\eta\right)&=\varpi\left[8\eta\varpi\left(4r\varpi^3-4\eta+2r^2\varpi^2\eta+3r^2\varpi^4\eta+12r\varpi^3\eta^2-12\eta^3\right)\right.\\ &\quad\left.+\left(4+3r^2\varpi^4+2r^2\varpi^2+12\eta^2\right)\left(4\varpi-r^2\varpi^5-2r^2\varpi^3+8r\varpi^2\eta+8r\eta+12\varpi\eta^2\right)\right]\ , &(52)\end{aligned}$$

while Einstein's equation (39) becomes

$$I\left(r,\varpi,\eta\right)r\frac{d}{dr}\varpi+J\left(r,\varpi,\eta\right)r\frac{d}{dr}\eta=K\left(r,\varpi,\eta\right)\ , \tag{53}$$

$$\begin{aligned} I\left(r,\varpi,\eta\right)&=r\eta\varpi^2\ , &(54)\\ J\left(r,\varpi,\eta\right)&=-2\eta\ , &(55)\\ K\left(r,\varpi,\eta\right)&=\tfrac{1}{2}r^2\varpi^2\left(1+\tfrac{1}{2}\varpi^2\right)+\eta^2-1\ . &(56)\end{aligned}$$

Numerical results

As a representative example with $\varpi > 0$, (53) and (49) were integrated numerically to obtain the results shown in the Figure, for data initialized as $\varpi|_{r=1} = 0.5$ and $\eta|_{r=1} = 1$.

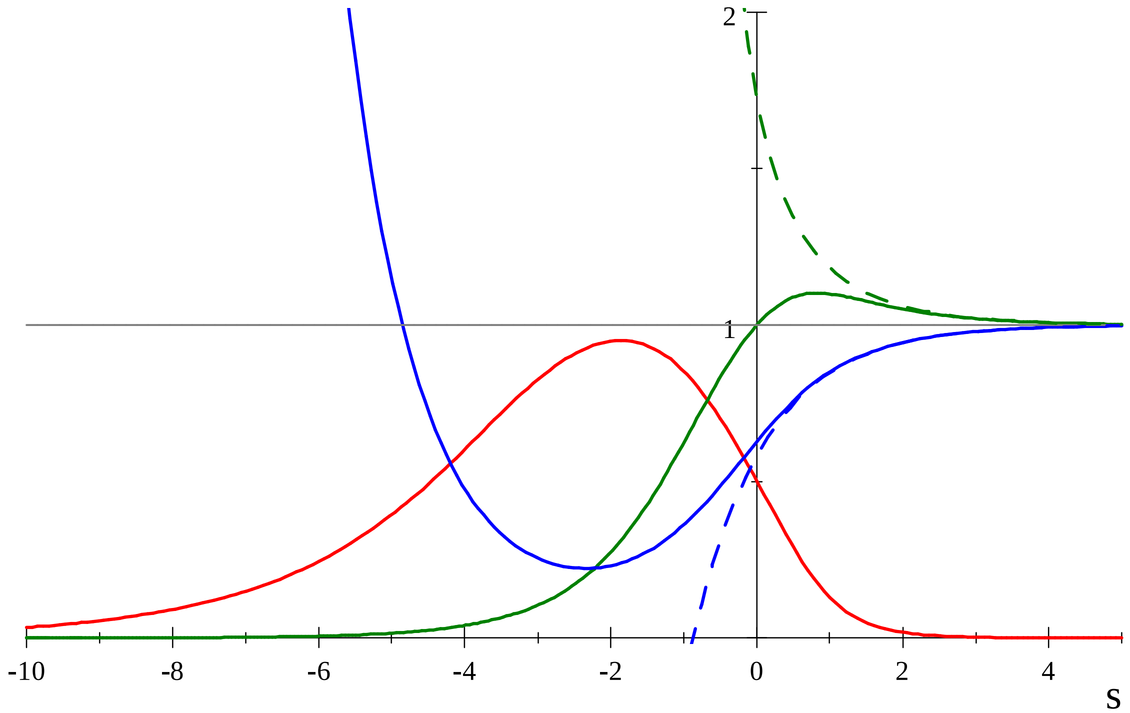

For initial values $\varpi(s)|_{s=0} = 0.5$ and $\eta(s)|_{s=0} = 1.0$, $d\phi/dr = \varpi/\eta$ is shown in red, $e^L = 1/\eta^2$ in green, and e^N in blue, where $r = e^s$. For comparison, Schwarzschild e^L and e^N are also shown as resp. green and blue dashed curves for the same $M \approx 0.21$.

Evidently it is true that $\eta(r) \neq \frac{1}{2}r\varpi^3(r)$ for this case, so $e^{N(r)}$ does not vanish for any $r > 0$ and there is no event horizon.

However, there is a geometric singularity at $r = 0$ with divergent scalar curvature: $\lim_{r\to 0} r^{3/2} R = const$. Since $R = -\Theta_\mu{}^\mu$, and $\lim_{r\to 0} \varpi$ is finite, this divergence in R comes from the last term in (44), which in turn comes from the second term in A, i.e. the covariant $\partial\phi\partial\phi\partial^2\phi$ in (33). In fact, it it not difficult to establish analytically for a class of solutions of the model, for which the example in the Figure is representative, the following limiting behavior holds.

$$\lim_{r\to 0} \left(e^{L/2}/\sqrt{r}\right) = \ell \ , \quad \lim_{r\to 0} \left(\sqrt{r} e^{N/2}\right) = n \ , \quad \lim_{r\to 0} \varpi = p \ , \quad \lim_{r\to 0} \left(\phi'/\sqrt{r}\right) = p\ell \ , \tag{57}$$

where ℓ, n, and p are constants related to the constant C in (42):

$$2C = 3np^2/\ell \ . \tag{58}$$

It follows that for solutions in this class,

$$\lim_{r\to 0} r^{3/2} R = pC/n \ . \tag{59}$$

For the example shown in the Figure: $\ell \approx 1.5$, $n \approx 0.086$, $p \approx 3.3$, $C \approx 0.94$, and $pC/n \approx 36$.

The energy contained in *only* the scalar field in the curved spacetime is given by

$$E_{\text{Galileon}} = \int_0^\infty \mathcal{H}(r)\,dr = \int_{-\infty}^\infty e^s \mathcal{H}(e^s)\,ds \ , \tag{60}$$

$$\mathcal{H}(r) \equiv 4\pi r^2 e^{L/2} e^{N/2} \Theta_t{}^t = 2\pi e^{2s} e^{L/2} e^{N/2} \varpi^2(s)\left(1+\tfrac{1}{2}\varpi^2(s)\right) - 4\pi e^s e^{N/2} \varpi^2(s) \tfrac{d}{ds}\varpi(s) \ . \tag{61}$$

For the above numerical example, the integrand $e^s\mathcal{H}(e^s)$ is shown in the following Figure.

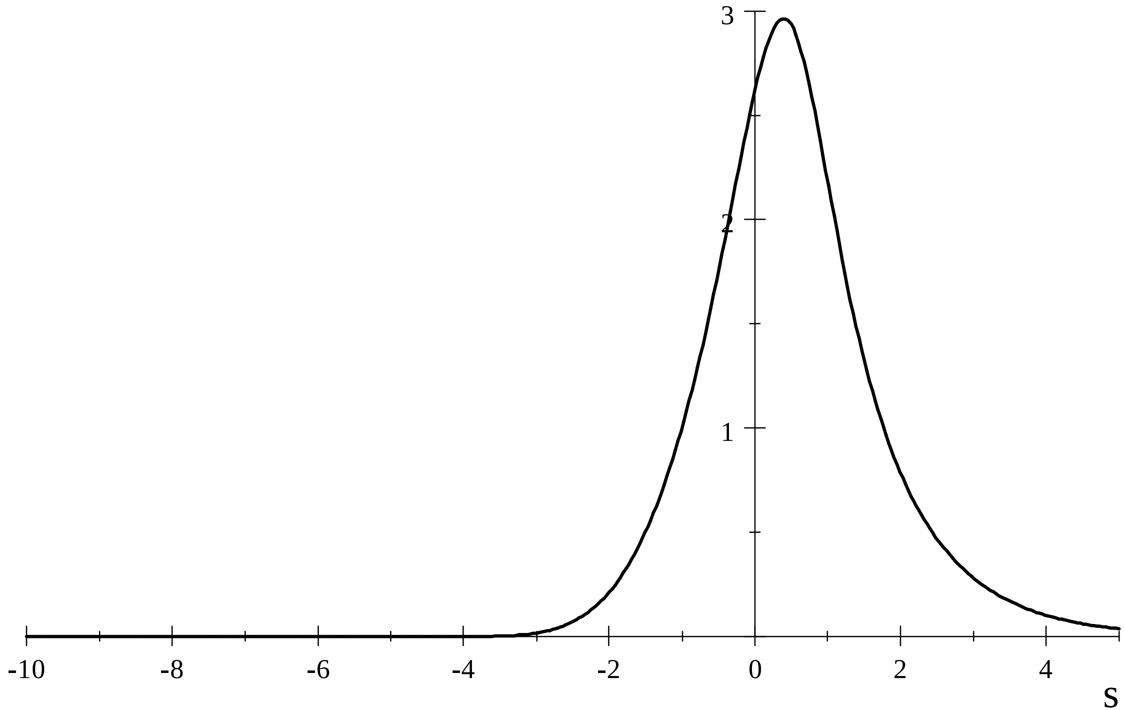

$e^s\mathcal{H}(e^s)$ for $\varpi(s)|_{s=0} = 0.5$ and $\eta(s)|_{s=0} = 1.0$, where $r = e^s$.

Evidently, E_{Galileon} is finite in this case. It is also clear from the Figures that the Galileon field has significant effects on the geometry in the vicinity of the peak of its radial energy density.

Other numerical examples

For the same $\eta|_{r=1} = 1$, further numerical results show there are also curvature singularities without horizons for smaller $\varpi|_{r=1} > 0$, but event horizons are present for larger scalar fields (roughly when $\varpi|_{r=1} > 2/3$). A more precise and complete characterization of the data set $\{\varpi|_{r=1}, \eta|_{r=1}\}$ for which there are naked singularities is given below, but it is already evident from the preceding remarks that the set has nonzero measure. Here are additional plots for $\eta(s)|_{s=0} = 1.0$ and various initial values $\varpi(s)|_{s=0}$. As before, $d\phi/dr = \varpi/\eta$ is shown in red, $e^L = 1/\eta^2$ in green, and e^N in blue, where $r = e^s$. For comparison, Schwarzschild e^L and e^N are also shown as resp. green and blue dashed curves for the same M, as given in the Figure labels.

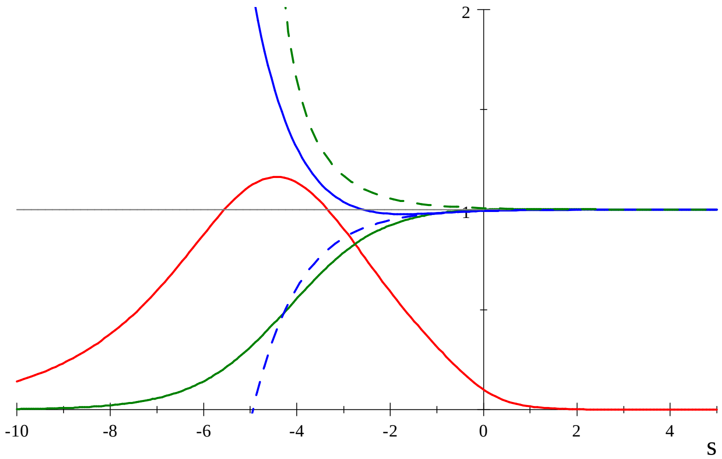

Initial values $\varpi(s)|_{s=0} = 0.100$ and $\eta(s)|_{s=0} = 1.00$
corresponding to $M = 0.00358$ and $C = 0.121$

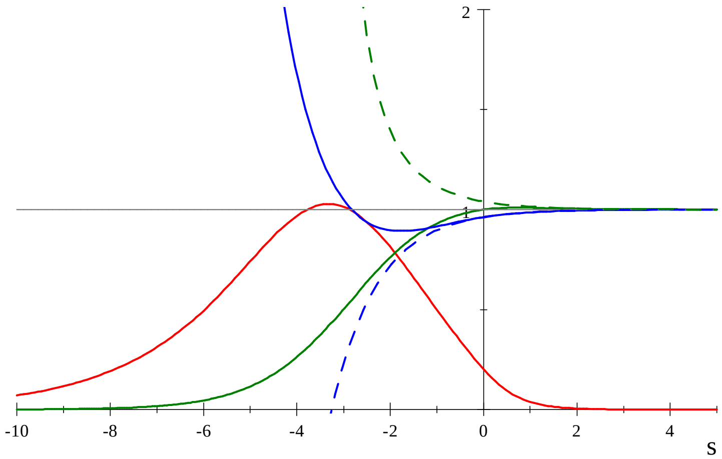

Initial values $\varpi(s)|_{s=0} = 0.200$ and $\eta(s)|_{s=0} = 1.00$
corresponding to $M = 0.0191$ and $C = 0.283$

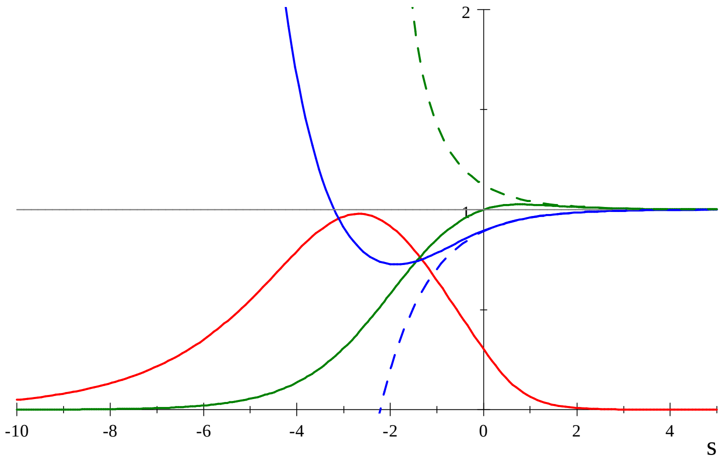

Initial values $\varpi(s)|_{s=0} = 0.300$ and $\eta(s)|_{s=0} = 1.00$
corresponding to $M = 0.0546$ and $C = 0.484$

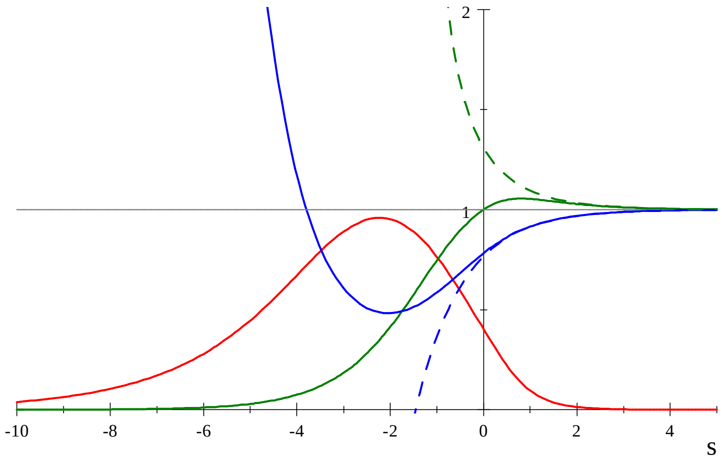

Initial values $\varpi(s)|_{s=0} = 0.400$ and $\eta(s)|_{s=0} = 1.00$
corresponding to $M = 0.117$ and $C = 0.710$

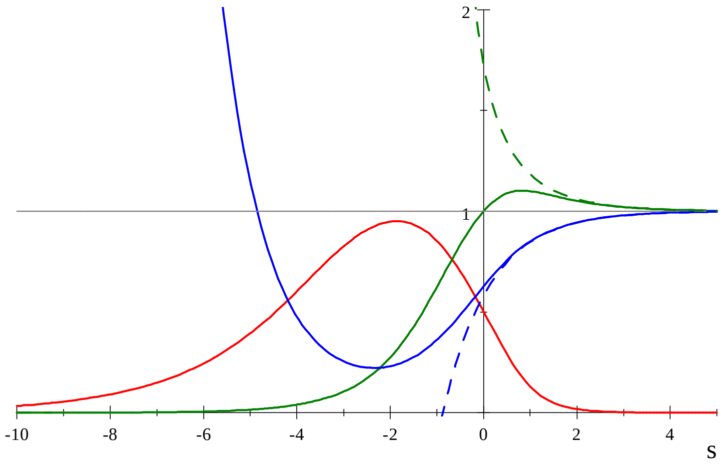

Initial values $\varpi(s)|_{s=0} = 0.500$ and $\eta(s)|_{s=0} = 1.00$
corresponding to $M = 0.209$ and $C = 0.936$

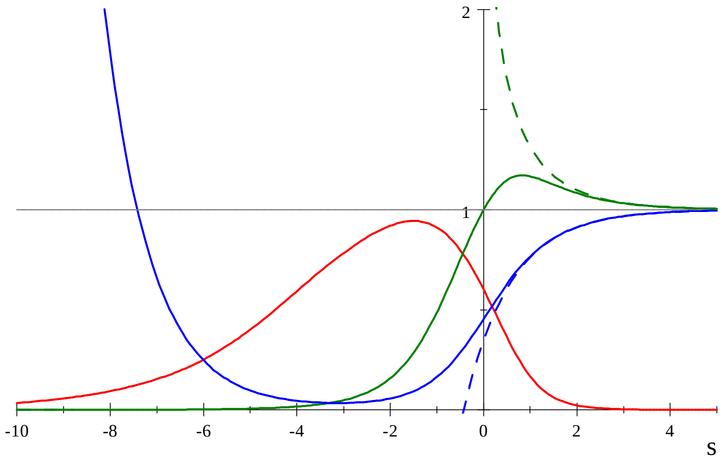

Initial values $\varpi(s)|_{s=0} = 0.600$ and $\eta(s)|_{s=0} = 1.00$
corresponding to $M = 0.326$ and $C = 1.13$

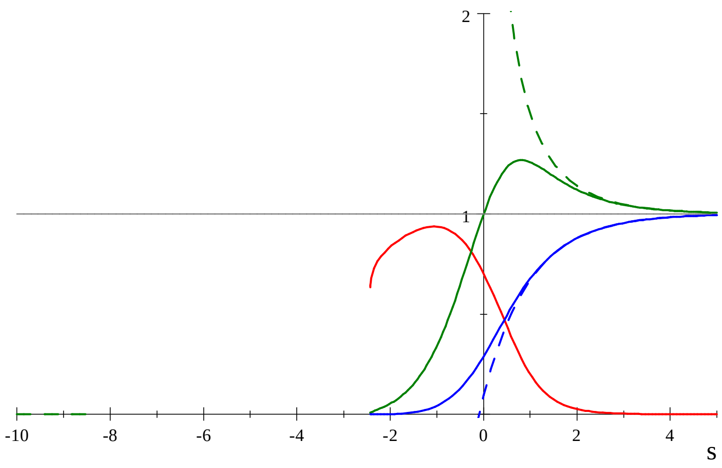

Initial values $\varpi(s)|_{s=0} = 0.700$ and $\eta(s)|_{s=0} = 1.00$
corresponding to $M = 0.453$ and $C = 1.26$

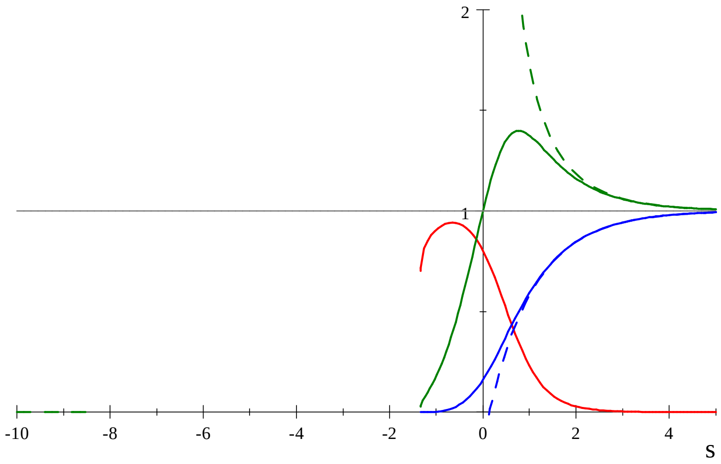

Initial values $\varpi(s)|_{s=0} = 0.800$ and $\eta(s)|_{s=0} = 1.00$
corresponding to $M = 0.573$ and $C = 1.32$

For each of the last two plots, the numerical integration of the coupled galileon-GR equations has encountered a mathematical (as opposed to physical?) singularity and terminated, resp. at $r \approx e^{-2.5} = 0.082$ and $r \approx e^{-1.3} = 0.27$, as is indicative of an horizon for which $e^N = 0$. This feature persists for initial data with larger values of $\varpi(s)|_{s=0}$, when $\eta(s)|_{s=0} = 1$.

Here are two more cases, just below and just above the point where horizons are formed. Again, for the second of these plots, the numerical integration of the coupled galileon-GR equations has encountered a mathematical singularity, and terminated at the point where $e^{N(r)}$ (blue curve) vanishes.

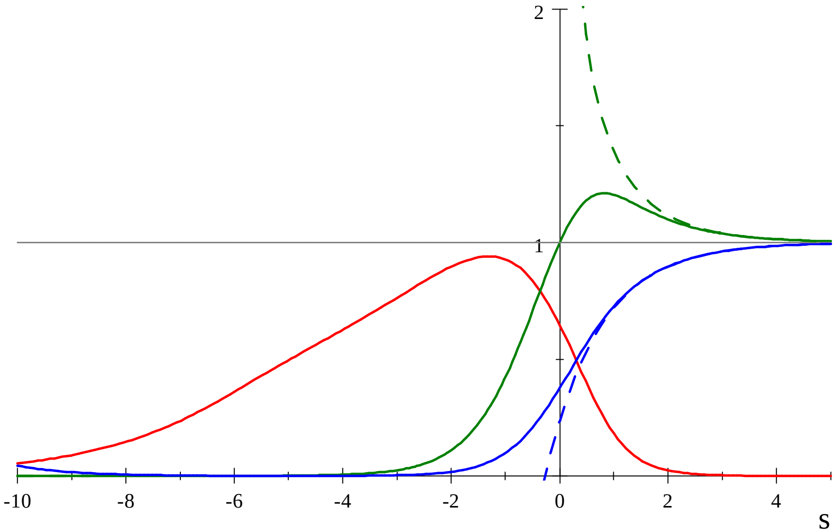

Initial values $\varpi(s)|_{s=0} = 0.645$ and $\eta(s)|_{s=0} = 1.00$ corresponding to $M = 0.383$ and $C = 1.199$

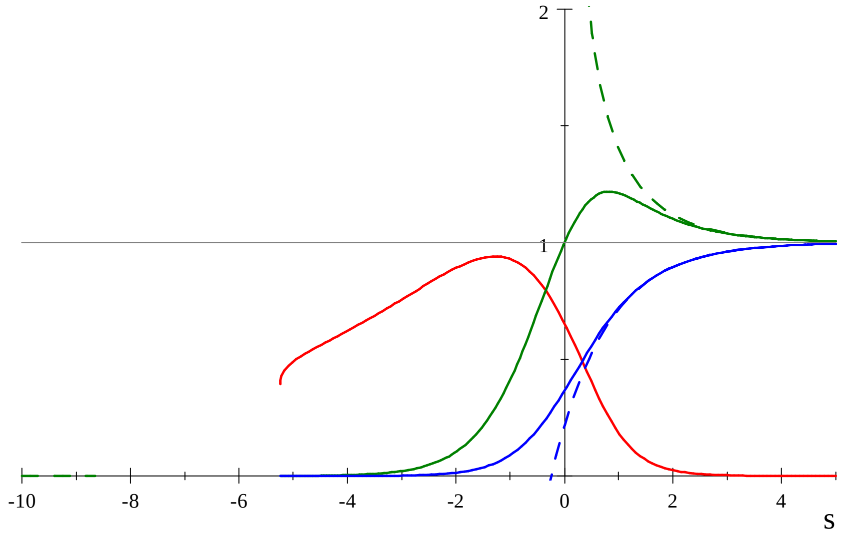

Initial values $\varpi(s)|_{s=0} = 0.652$ and $\eta(s)|_{s=0} = 1.00$ corresponding to $M = 0.392$ and $C = 1.209$

A useful test for an horizon is provided by the numerator of e^N in (45). Define the discriminant

$$disc\,(r) = 1 - \frac{r\ \varpi\,(r)^3}{2\ \eta\,(r)}\ . \tag{62}$$

Should this vanish at some radius for which $\eta\,(r)$ is finite, then at that radius $e^{N(r)} = 0$, thereby indicating an horizon at that radius. The *critical case*, separating solutions with naked singularities from those with event horizons, has the small r limiting behavior $\eta\,(r) \underset{r\to 0}{\sim} r\ \varpi^3\,(r)$, such that the discriminant $disc \underset{r\to 0}{\sim} \frac{1}{2}$ as illustrated here for specific data.

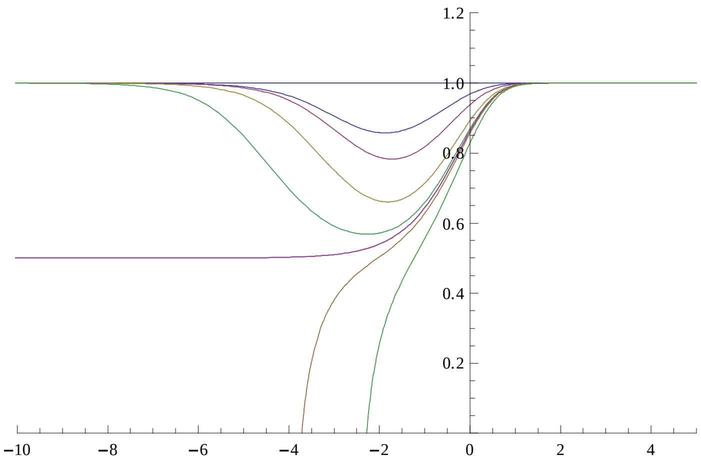

The discriminant $disc = 1 - \frac{1}{2} r \varpi^3 / \eta$ versus $s = \ln r$ for various $\varpi|_{r=1}$ (namely, 0.4, 0.5, 0.6, 0.64, critical, 0.66, and 0.7) with $\eta|_{r=1} = 1$. The critical initial value for the separatrix, for which $disc \underset{r \to 0}{\sim} 1/2$, is $\varpi|_{r=1} = 0.6500 \cdots$.

For initial data giving rise to naked singularities, $disc > 1/2$ (cf. the upper curves in the figure above), while for data leading to horizons, e^N vanishes at the horizon radius, and therefore at that radius $disc = 0$ (cf. the lower two curves in the figure). When the limiting critical behavior $\eta\,(r) \underset{r \to 0}{\sim} r\ \varpi^3\,(r)$ is inserted into the differential equations (53) and (49) we find the power law behavior:

$$\eta_{\rm critical}\,(r) \underset{r \to 0}{\sim} c^3 r^{-4/5}\ , \quad \varpi_{\rm critical}\,(r) \underset{r \to 0}{\sim} c r^{-3/5}\ , \quad \phi'_{\rm critical}\,(r) \underset{r \to 0}{\sim} \frac{r^{1/5}}{c^2}\ . \tag{63}$$

Moreover, critical cases are easily determined numerically for various initial data, $\{\varpi(s)|_{s=0}\,,\ \eta(s)|_{s=0}\}$, thereby allowing determination of a curve that separates the open set of initial data that exhibits naked singularities from the set that exhibits event horizons.

Censored and naked phases

The situation for a portion of the initial data plane is as follows.

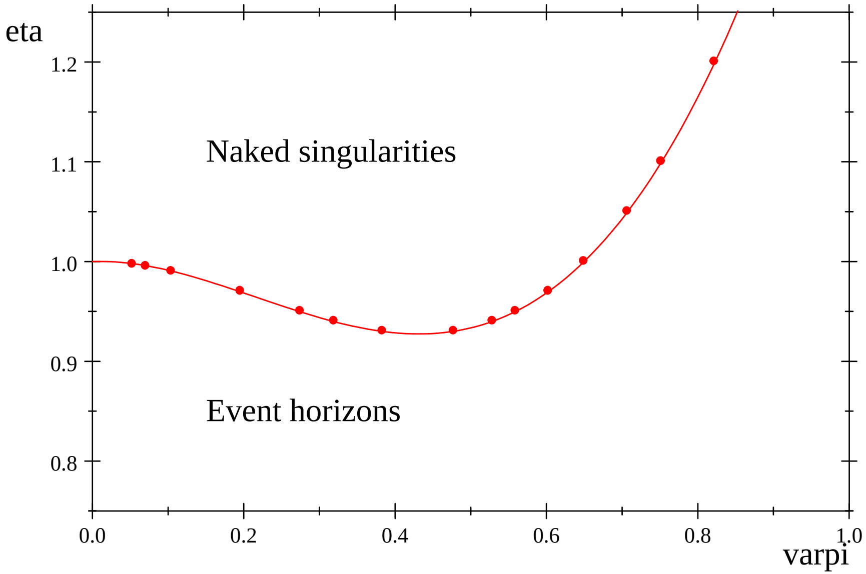

$\left(\varpi|_{r=1}, \eta|_{r=1}\right)$ boundary separating initial data that exhibit naked singularities from data that exhibit horizons. The curve is a fourth-order polynomial fit to the numerically computed critical points (dots), namely, $\eta_{\text{fit}}(\varpi) = 1 + 0.0255538\varpi - 1.34405\varpi^2 + 2.20589\varpi^3 - 0.304933\varpi^4$.

This shows naked singularities for the model exist for an initial data set of non-zero measure, and are actually encountered for a significant portion of the initial data plane.

A similar demarcation between naked/censored solutions can be presented in terms of asymptotic $r \to \infty$ data instead of initial $r = 1$ data. With M and C defined as in (46), (47), and (48), we find the following curve separating the two types of solutions. Solutions for points above the red curve have naked singularities, while solutions for points below that curve have event horizons.

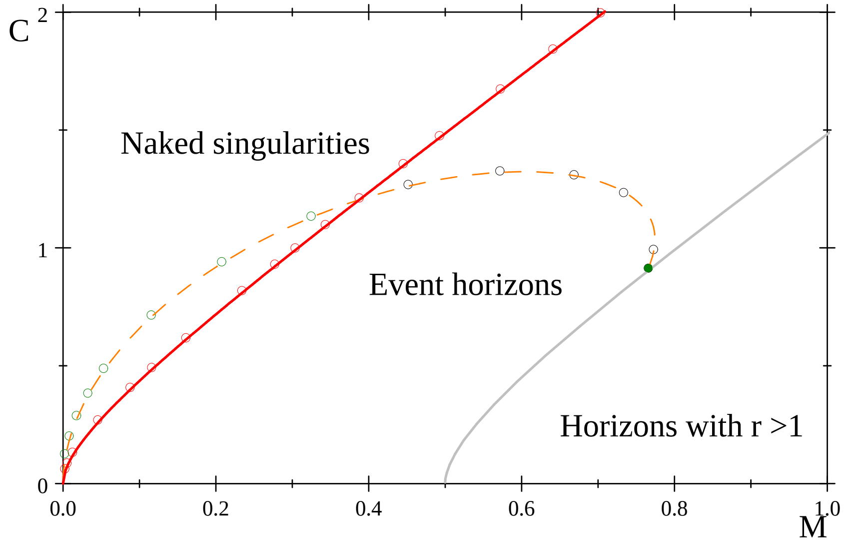

Computed points (red circles) and an interpolating curve (solid red) separating the $r \to \infty$ asymptotic data for solutions with naked singularities from that for solutions with event horizons.

By imposing the same $\eta(s)|_{s=0}$ initial condition for various values of $\varpi(s)|_{s=0}$, the numerical data also shows that the corresponding $C(M)$ has a local maximum, and hence $M(C)$ becomes double-valued near that point.

For example, when $\eta(s)|_{s=0} = 1$ the local maximum for $C(M)$ is near $\varpi(s)|_{s=0} \approx 0.78$. By examining larger $\varpi(s)|_{s=0}$ for the same $\eta(s)|_{s=0}$, it is apparent that $C(M)$ can also be double-valued. All this is evident in a parametric plot of the corresponding (C, M) points on the data plane. For example, for $\eta(s)|_{s=0} = 1$ and various $\varpi(s)|_{s=0} \in \left[0.1,\ 1.259\,92 = \sqrt[3]{2}\right]$, we find the naked (green circle) and censored (black circle) data as included in the last figure, with a fitted interpolating curve (orange dashes) connecting the computed points. In this numerical analysis, care should be taken not to have $\varpi(s)|_{s=0}$ larger than $\sqrt[3]{2\,\eta(s)|_{s=0}}$ because otherwise this would place data initialized at $r = 1$ *within* the horizon. The horizon is exactly at the radius $r = 1$ when $\varpi(s)|_{s=0} = \sqrt[3]{2\,\eta(s)|_{s=0}}$. The gray curve in the last figure is the image of $\varpi(s)|_{s=0} = \sqrt[3]{2\,\eta(s)|_{s=0}}$ on the (M, C) plane. Points below this gray curve can be investigated numerically using Schwarzshild coordinates but only if the initial data is specified for $r > 1$, i.e. *outside* the horizon. (Also note the portion of the initial data plane shown in the previous figure lies entirely above the curve $\eta(s)|_{s=0} = \frac{1}{2}\,\varpi^3(s)|_{s=0}$, so all initial data points in that figure lie outside of any horizons.)

Conclusions

In conclusion, as previously emphasized by many authors it would be interesting to search for evidence of galileons at all distance scales, including galactic and sub-galactic, as well as cosmological. Perhaps a combination of trace couplings and various galileon terms will ultimately lead to a realistic physical model. In particular, it is important to investigate the stability of galileon solutions and to consider the dynamical evolution of generic galileon and other matter field initial data to determine under what physical conditions naked singularities might actually form.

Acknowledgements: Thank you for the opportunity to visit FAU and present this material. This research was supported by a University of Miami Cooper Fellowship, and by NSF Awards PHY-0855386 and PHY-1214521.

References

[1] S. A. Appleby and E. V. Linder, "Galileons on trial" arXiv:1204.4314

[2] C. Charmousis, B. Goutéraux, and E. Kiritsis, "Higher-derivative scalar-vector-tensor theories: black holes, Galileons, singularity cloaking and holography" arXiv:1206.1499 [hep-th]

[3] T. Chaundy, *The Differential Calculus*, The Clarendon Press, Oxford (1935).

[4] M. W. Choptuik, "Universality and Scaling in Gravitational Collapse of a Massless Scalar Field" Phys. Rev. Lett 70 (1993) 9-12

[5] M. W. Choptuik, E. W. Hirschmann, S. L. Liebling, and F. Pretorius, "Critical collapse of the massless scalar field in axisymmetry" Phys. Rev. D68 (2003) 044007, arXiv:gr-qc/0305003.

[6] P. Creminelli, K. Hinterbichler, J. Khoury, A. Nicolis, and E. Trincherini, "Subluminal Galilean Genesis" arXiv:1209.3768

[7] T. Curtright, "Galileons and Naked Singularities" Phys. Lett. B716 (2012) 366-369, arXiv:1208.1205 [hep-th]

[8] T. Curtright and D. Fairlie, "Geons of Galileons" Phys. Lett. B716 (2012) 356-360, arXiv:1206.3616 [hep-th]

[9] C. Deffayet, S. Deser, and G. Esposito-Farese, "Generalized Galileons: All scalar models whose curved background extensions maintain second-order field equations and stress tensors" Phys. Rev. D80 (2009) 064015, arxiv:0906.1967 [hep-th]

[10] C. Deffayet, G. Esposito-Farese, and A. Vikman, "Covariant Galileon" Phys. Rev. D79 (2009) 084003, arXiv:0901.1314 [hep-th]

[11] G. H. Derrick, "Comments on Nonlinear Wave Equations as Models for Elementary Particles" J. Math. Phys. 5 (1964) 1252-1254

[12] C. de Rham, “Galileons in the Sky” arXiv:1204.5492 [astro-ph.CO] to appear in Compt. Rend. Acad´emie Sci. (2012)

[13] G. R. Dvali, G. Gabadadze, and M. Porrati, “4-D gravity on a brane in 5-D Minkowski space” Phys. Lett. B 485 (2000) 208 [arXiv:hep-th/0005016]; M. A. Luty, M. Porrati and R. Rattazzi, “Strong interactions and stability in the DGP model” JHEP 0309 (2003) 029 [arXiv:hep-th/0303116]; A. Nicolis and R. Rattazzi, “Classical and quantum consistency of the DGP model” JHEP 0406 (2004) 059 [arXiv:hep-th/0404159]

[14] S. Endlich, K. Hinterbichler, L. Hui, A. Nicolis, and J. Wang, “Derrick’s theorem beyond a potential” JHEP 05 (2011) 73, arXiv:1002.4873 [hep-th]; A. Padilla, P.M. Saffin, and S.-Y. Zhou, “Multi-galileons, solitons and Derrick’s theorem” Phys. Rev. D83 (2011) 045009, arXiv:1008.0745 [hep-th]

[15] D. B. Fairlie, “Comments on Galileons” J. Phys. A44 (2011) 305201, arXiv:1102.1594 [hep-th]

[16] D. B. Fairlie, “Implicit solutions to some Lorentz invariant non-linear equations revisited” J. Nonlinear Math. Phys. **12** (2005) 449-456 [math-ph/0412005]

[17] D. B. Fairlie and J. Govaerts, “Universal field equations with reparametrisation invariance” Phys. Lett. B 281 (1992) 49-53 [arXiv:hep-th/9202056]

[18] D. B. Fairlie and J. Govaerts, “Euler hierarchies and universal equations” J. Math. Phys. 33 (1992) 3543-3566 [arXiv hep-th/9204074]

[19] D. B. Fairlie and J. Govaerts, “Linearisation of Universal Field Equations” J. Phys. A26 (1993) 3339-3347 [arXiv:hep-th/9212005]

[20] D. B. Fairlie, J. Govaerts, and A. Morozov “Universal field equations with covariant solutions” Nucl. Phys. B373 (1992) 214-232 [arXiv hep-th/9110022]

[21] P. G. O. Freund and Y. Nambu, "Scalar field coupled to the trace of the energy-momentum tensor" Phys. Rev. 174 (1968) 1741-1743. Also see Appendix II in R. H. Kraichnan, "Special-Relativistic Derivation of Generally Covariant Gravitation Theory" Phys. Rev. 98 (1955) 1118-1122, as well as S. Deser and L. Halpern "Self-coupled scalar gravitation" Gen. Rel. Grav. 1 (1970) 131-136. The history of this idea is traced in K. Hinterbichler, "Theoretical Aspects of Massive Gravity" Rev. Mod. Phys. 84 (2012) 671-710, arXiv:1105.3735 [hep-th]

[22] G. Gabadadze, K. Hinterbichler, and D. Pirtskhalava, "Classical Duals of Derivatively Self-Coupled Theories" arXiv:1202.6364 [hep-th]

[23] G. L. Goon, K. Hinterbichler, M. Trodden, "Stability and superluminality of spherical DBI galileon solutions" Phys. Rev. D83 (2011) 085015 arXiv:1008.4580 [hep-th]

[24] G. W. Horndeski, "Second-order scalar-tensor field equations in a four-dimensional space" Int. J. Theor. Physics 10 (1974) 363-384. Also see C. Deffayet, Xian Gao, D. A. Steer, and G. Zahariade, "From k-essence to generalised Galileons" Phys. Rev. D84 (2011) 064039 arXiv:1103.3260 [hep-th]

[25] L. Iorio, "Constraints on Galileon-induced precessions from solar system orbital motions" JCAP 07 (2012) 001

[26] R. Jackiw and S.-Y. Pi, "Tutorial on Scale and Conformal Symmetries in Diverse Dimensions" J. Phys. A44 (2011) 223001, arXiv:1101.4886 [math-ph], and references therein.

[27] L. Meyer, A. M. Ghez, R. Schödel, S. Yelda, A. Boehle, J. R. Lu, T. Do, M. R. Morris, E. E. Becklin, and K. Matthews, "The Shortest-Known–Period Star Orbiting Our Galaxy's Supermassive Black Hole" Science 338 (2012) 84-87, DOI: 10.1126/science.1225506

[28] M. Morris, L. Meyer, and A. Ghez, "Galactic Center Research: Manifestations of the Central Black Hole" arXiv:1207.6755 [astro-ph.GA]

[29] R. Penrose, "The Question of Cosmic Censorship" J. Astrophys. Astr. 20 (1999) 233–248

[30] Horizon-less solutions with naked singularities have also appeared in recent studies on solutions to higher dimensional Einstein equations in vacuum, suitable for describing intersecting brane solutions in string/M theory. In particular, see S. K. Rama, “Static brane–like vacuum solutions in $D \geq 5$ dimensional spacetime with positive ADM mass but no horizon” arXiv:1111.1897 [hep-th]

[31] In the context of a different Galileon model, numerical evidence of naked singularities is also mentioned in passing by M. Rinaldi, “Galileon Black Holes” arXiv:1208.0103v1 [gr-qc]

[32] T. P. Singh, “Gravitational Collapse, Black Holes and Naked Singularities” J. Astrophys. Astr. 20 (1999) 221–232 [arXiv:gr-qc/9805066]

[33] T. H. R. Skyrme, “A unified field theory of mesons and baryons” Nucl. Phys. 31 (1962) 556-569

[34] R. C. Tolman, *Relativity, Thermodynamics, and Cosmology*, Dover Publications (1987)

[35] A. I. Vainshtein, “To the problem of nonvanishing gravitation mass” Phys. Lett. B 39 (1972) 393-394

[36] K. S. Virbhadra, D. Narasimha, and S. M. Chitre, “Role of the scalar field in gravitational lensing” Astron. Astrophys. 337 (1998) 1-8; K. S. Virbhadra and G. F. R. Ellis, “Gravitational lensing by naked singularities” Phys. Rev. D 65 (2002) 103004; K. S. Virbhadra and C. R. Keeton, “Time delay and magnification centroid due to gravitational lensing by black holes and naked singularities” Phys. Rev. D 77 (2008) 124014, arXiv:0710.2333

[37] R. Wald, “Gravitational Collapse and Cosmic Censorship” [arXiv:gr-qc/9710068]

[38] J. A. Wheeler, “Geons” Phys. Rev. 97 (1955) 511-536. Also see P. R. Anderson and D. R. Brill, “Gravitational Geons Revisited” Phys. Rev. D56 (1997) 4824-4833, arXiv:gr-qc/9610074